Int J Earth Sci (Geol Rundsch)
DOI 10.1007/s00531-012-0822-z

ORIGINAL PAPER

Seepage of methane at Jaco Scar, a slide caused by seamount subduction offshore Costa Rica

Susan Mau · Gregor Rehder · Heiko Sahling · Tina Schleicher · Peter Linke

Received: 10 October 2011 / Accepted: 2 September 2012

Abstract Methane (CH_4) concentrations and CH_4 stable carbon isotopic composition ($\delta^{13}C_{CH_4}$) were investigated in the water column within Jaco Scar. It is one of several scars formed by massive slides resulting from the subduction of seamounts offshore Costa Rica, a process that can open up structural and stratigraphical pathways for migrating CH_4. The release of large amounts of CH_4 into the adjacent water column was discovered at the outcropping lowermost sedimentary sequence of the hanging wall in the northwest corner of Jaco Scar, where concentrations reached up to 1,500 nmol L^{-1}. There CH_4-rich fluids seeping from the sedimentary sequence stimulate both growth and activity of a dense chemosynthetic community. Additional point sources supplying CH_4 at lower concentrations were identified in density layers above and below the main plume from light carbon isotope ratios. The injected CH_4 is most likely a mixture of microbial and thermogenic CH_4 as suggested by $\delta^{13}C_{CH_4}$ values between −50 and −62 ‰ Vienna Pee Dee Belemnite. This CH_4 spreads along isopycnal surfaces throughout the whole area of the scar, and the concentrations decrease due to mixing with ocean water and microbial oxidation. The supply of CH_4 appears to be persistent as repeatedly high CH_4 concentrations were found within the scar over 6 years. The maximum CH_4 concentration and average excess CH_4 concentration at Jaco Scar indicate that CH_4 seepage from scars might be as significant as seepage from other tectonic structures in the marine realm. Hence, taking into account the global abundance of scars, such structures might constitute a substantial, hitherto unconsidered contribution to natural CH_4 sources at the seafloor.

Keywords Submarine slide · Cold seeps · Stable carbon isotopes · Methane · Seamount subduction · Costa Rican fore-arc

Electronic supplementary material The online version of this article (doi:10.1007/s00531-012-0822-z) contains supplementary material, which is available to authorized users.

S. Mau · G. Rehder · H. Sahling · T. Schleicher · P. Linke
Sonderforschungsbereich 574, University of Kiel, Kiel, Germany

S. Mau (✉)
Max-Planck-Institute for Marine Microbiology, Celsiusstr. 1, 28359 Bremen, Germany
e-mail: smau@mpi-bremen.de

G. Rehder
Leibniz Institute for Baltic Sea Research Warnemünde, Seestr. 15, 18119 Rostock, Germany

H. Sahling
Department of Geosciences, MARUM Center for Marine Environmental Sciences, Klagenfurter Str., 28359 Bremen, Germany

T. Schleicher
Department of Bioinformatics, University of Würzburg, Am Hubland, 97074 Würzburg, Germany

P. Linke
GEOMAR – Helmholtz Centre for Ocean Research Kiel, Wischhofstr. 1-3, 24148 Kiel, Germany

Introduction

Methane is the most common "geogenic gas," and attempts of quantification (Cranston et al. 1994; Hovland et al. 1997; Judd et al. 1997, 2002; Hornafius et al. 1999; Reeburgh 2007) have illustrated the significance of this gas to the global carbon budget (Judd et al. 2002). CH_4 is generated in sediments by the decomposition of organic matter buried when the sediments were deposited. Microbial CH_4 is produced by

Published online: 28 September 2012

methanogenesis at relatively shallow sediment depths, whereas thermogenic CH_4 is formed in high temperature and pressure conditions in depths greater than one kilometer (Tissot and Welte 1984). Buoyancy-triggered advection and pressure gradients transport the gas toward the earth's surface. On the way, several processes decrease the amount of CH_4 that reaches the sediment–water interface. CH_4 can be removed by hydrate formation in the gas hydrate stability zone (Reed et al. 1990). Just below the sediment surface, a large fraction is anaerobically oxidized, leading to the precipitation of authigenic carbonates (Kulm et al. 1986) and providing energy for vent-specific biota (Sibuet and Olu 1998). Most vent fauna rely on hydrogen sulfide produced by anaerobic oxidation of CH_4 instead of directly using CH_4 as energy source (Fisher 1990). If the CH_4 flux to the ocean is not completely exhausted by these processes, a fraction of the CH_4 is emitted into the water column. This CH_4 can be emitted either dissolved in fluids or, in case of over-saturation, in form of gas bubbles (Valentine et al. 2001; Judd and Hovland 2007; Reeburgh 2007).

Seep-derived CH_4 in the water column is further diluted due to mixing with ocean water, and the concentration also decreases due to microbial aerobic CH_4 oxidation in most parts of the ocean. Only in anoxic basins does anaerobic oxidation of CH_4 become important (Reeburgh 2007). The stable carbon isotopic composition of CH_4 can be used to discriminate between mixing and microbial oxidation, because dilution results in a mixed isotope ratio from background CH_4 and seep-derived CH_4. In contrast, oxidation of CH_4 leaves the residual CH_4 enriched in ^{13}C (Barker and Fritz 1981; Damm and Budeus 2003). This difference permits the determination of which of the two pathways dominates and of what kind of species (CO_2 or CH_4) are supplied to the ocean carbon pool in a specified space and time frame.

Natural CH_4 seeps occur near shore, at continental shelves, and in the deep ocean (Judd et al. 2002; Judd and Hovland 2007). The determination of the extent and source strength of the various seep structures is one of the most significant hurdles to estimate the role of natural seepage in the global CH_4 budget (Kvenvolden et al. 2001; Reeburgh 2007). Up to date, CH_4 emission into the water column from mud extrusions (Cita et al. 1995; Henry et al. 1996; Ginsburg et al. 1999; Lein et al. 1999; Kopf and Behrmann 2000; Damm and Budeus 2003; Haese et al. 2003; Mau et al. 2006; Sahling et al. 2009), anticlines (Suess et al. 1998; Clark et al. 2000; Wiedicke et al. 2002; Heeschen et al. 2005; Faure et al. 2010), canyons (Dia et al. 1993; Olu et al. 1996a; Suess et al. 1998; von Rad et al. 2000; Valentine et al. 2001), slides (Dia et al. 1993; Olu et al. 1996a), and paleo-deltas (Sahling et al. 2008a; Schmale et al. 2010) has been reported. Most of these structures are connected to faults which are prominent pathways for rising fluids (King 1986; Judd et al. 2002).

Although submarine slides commonly occur along continental margins, little is known about CH_4 seepage from these structures. In this paper, we report on CH_4 seepage from a slide offshore Costa Rica (Figs. 1, 2) formed by seamount subduction (Ranero and von Huene 2000). More than 45,000 seamounts are estimated to occur worldwide (Etnoyer et al. 2010), whose life spans end when they reach a subduction zone or when their host ocean basin closes due to the collision of two continental plates (Staudigel and Clague 2010). During subduction, seamounts intercept and destroy the frontal prism while being carried down the subduction zone. Afterward, the prism re-grows rapidly to its former extent, but tracks in the form of deeply cut grooves mark the further path of the seamount on the continental margin. Such subducted seamounts form circular uplifts with steep scars on their seaward side caused by failure of oversteepened sediments (von Huene et al. 2000; Hühnerbach et al. 2005) (Fig. 1). A number of steep scars were discovered offshore Costa Rica and elsewhere along the Middle American Pacific continental margin by high-resolution bathymetric mapping (Ranero and von Huene 2000; von Huene et al. 2000; Harders et al. 2011). Tracks of subducting seamounts on continental margins were also reported from the Aleutian subduction zone (Suess et al. 1998), the Japan Trench (Lallemand and Le Pichon 1987), the New Hebrides subduction zone (Collot and Fisher 1989), and the Tonga Trench (Ballance et al. 1989). The process of seamount subduction creates possible pathways for rising fluids and gas (Sahling et al. 2008b) as it involves formation of faults and cutting of upper slope sediments due to slides (Ranero and von Huene 2000; von Huene et al. 2000) from which accumulated CH_4 discharges.

We investigated CH_4 concentrations and the carbon isotopic signature of seep-derived CH_4 within the area of Jaco Scar, one of the prominent slides formed by seamount subduction offshore Costa Rica (Figs. 1, 2). Highest CH_4 concentrations of all water column stations studied during the PAGANINI expedition in 1999 (SO144, CTD02) (Bohrmann et al. 2002) were obtained inside Jaco Scar. Based on these primary data, high-resolution sampling of the water column was conducted to identify source and fate of CH_4 in the scar. The main venting area within Jaco Scar was further characterized by quantitative video analysis. Finally, we compared maximum CH_4 concentration and average excess CH_4 concentration of Jaco Scar with other natural sources of CH_4 in order to identify the significance of scars as natural CH_4 seeps in the marine realm.

Methods

CH_4 concentration and isotope ratios were measured in water samples at 12 different locations within the area

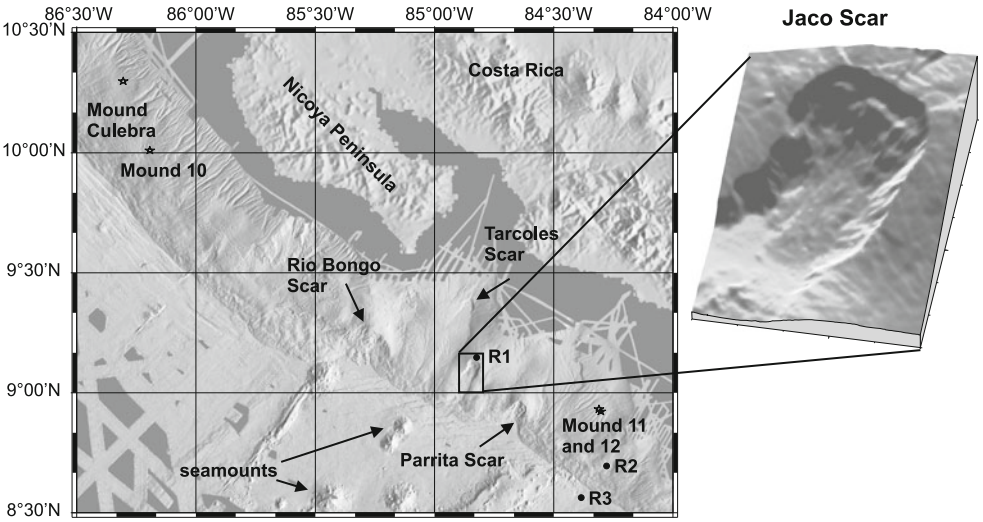

Fig. 1 Location of Jaco Scar at the continental margin off Costa Rica and a close-up of the scar. Other scars (pointed out by *arrows*) and CH_4-emitting mud extrusions (mounds = *stars*) along this part of the continental margin, which are referred to in the text, are also indicated. *R1*, *R2*, and *R3* represent reference stations

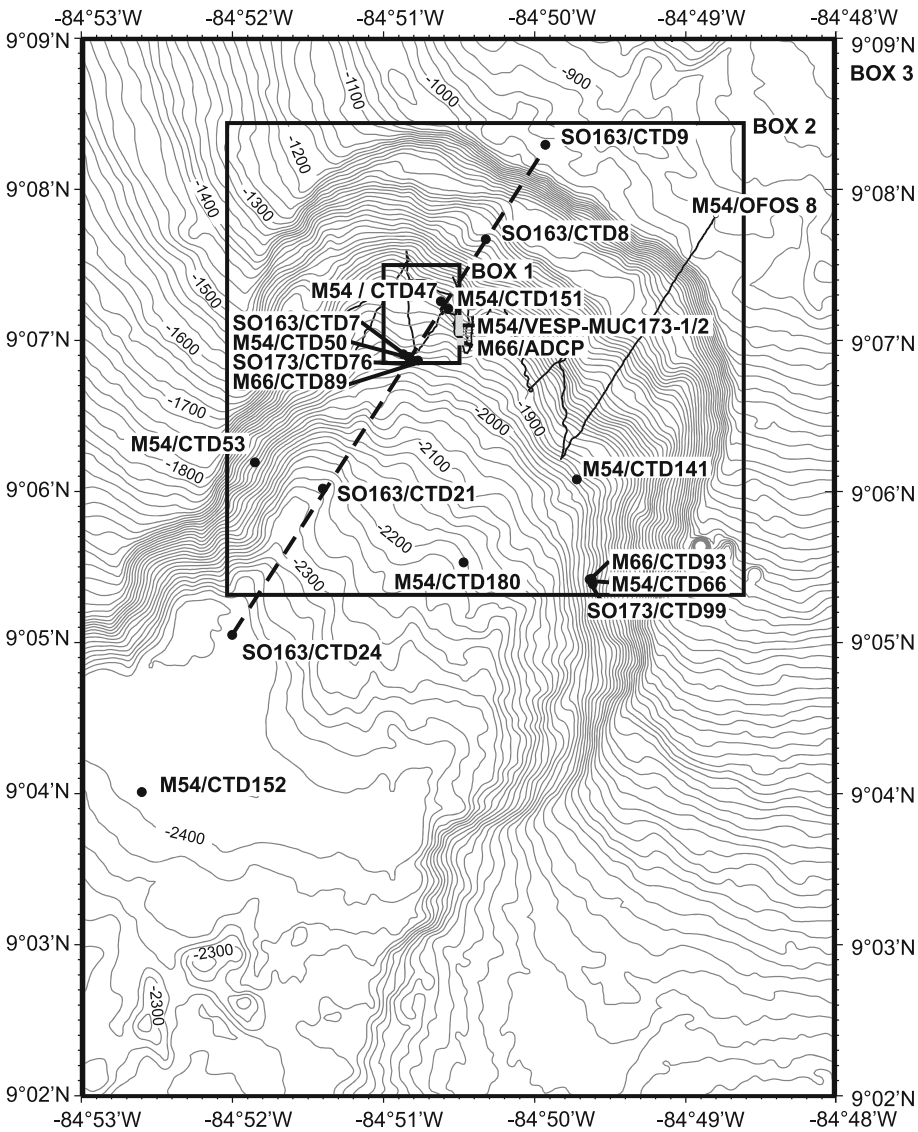

Fig. 2 Sampling stations at Jaco Scar are marked by *filled circles*. The labels of the stations indicate the time of sampling: SO163—April/May 2002; M54—August/September 2002; SO173—September 2003; M66—October 2005; and the sampling method: CTD—hydrocast sampling; VESP-MUC—video-guided sampling; ADCP—current record. *Box 1* displays the area where highest CH_4 concentrations were found, *box 2* the surrounding area of high CH_4 concentration (excluding *box 1*), and *box 3* the whole area of the map with CH_4 concentrations slightly above background CH_4 concentrations (excluding *box 1* and *2*). The seafloor survey with camera sled OFOS (M54/OFOS8) is displayed as *thin line* and the stations used for the contour plot of Fig. 5a are connected by a *thick*, *dashed line*

comprising Jaco Scar (Fig. 2). Reference stations R1, R2, and R3 are situated above the scar and farther away at the Costa Rican margin as illustrated in Fig. 1. Seawater samples were collected during cruises of research project SFB 574 "Volatiles and Fluids in Subduction Zones" at the University of Kiel, Germany, in April/May 2002 (SO163-2), August/September 2002 (M54-2/3), September 2003 (SO173-3/4), and October 2005 (M66-2). Reference station R1 was sampled during M54-2/3; R2 and R3 were sampled during SO163-2. In addition, an upward-looking Acoustic Doppler Current Profiler (ADCP) was deployed during M66-2.

Water samples for CH_4 analyses were collected by CTD/rosette and by a video-guided VEnt SamPler mounted to a modified MUltiCorer frame (VESP-MUC). Water samples taken by CTD/rosette were collected with decreasing height above the seafloor. Samples closest to the seafloor were taken at about 10–20 m above bottom. In contrast, the VESP-MUC was towed approximately 2–3 m above the seafloor and was deployed if signs of seepage became visible, for example, clam colonies, microbial mats, or carbonate crusts. The VESP-MUC consists of five 5-L Niskin-type water bottles (HYDRO-BIOS) (Linke et al. 1994). The ship's coaxial cable was used for bidirectional transmission of the video images, commands, data, and power supply of the underwater units (ADITEC/SCHOLZ).

For CH_4 analyses aboard, a modification (Rehder et al. 1999) of the vacuum degassing method described by Lammers and Suess (1994) was used. This method requires knowledge of the dissolved O_2 concentration, which was determined by Winckler titration (Grasshoff et al. 1997) in addition to the O_2 sensor of the CTD. CH_4 analyses of two series of samples from a single hydrocast yielded a precision of ±10 % for samples with CH_4 concentration <2 nmol L^{-1} and ±5 % for CH_4 concentration >2 nmol L^{-1}.

The remainder of the extracted gas from the vacuum degassing method was transferred to an evacuated 20-mL vial, preserved with 7 mL of saturated $HgCl_2$ solution, and stored for shore-based concentration and isotope ratio analysis. CH_4 and C_2H_6 concentrations of gas samples taken near the source were analyzed about 4 months after the M54/2&3 cruise using standard GC techniques (Shimadzu GC 14A). CH_4 concentrations measured on board and on shore deviated by less than ±1 %. Furthermore, gas samples were analyzed by isotope-ratio-monitoring gas chromatography/mass spectrometry (irm-GC/MS, Finnigan MAT 253). In preparation, aliquots of gas samples were purged using $Mg(ClO_4)_2$ and NaOH for purification and CO_2 removal, and a HayeSep D trap in an ethanol bath at −110 °C for cryofocussing. The CH_4 was separated by gas chromatography using a 30-m, 0.32-mm i.D. Poraplot Q capillary column run isothermally at 50 °C, and then oxidized to CO_2 in a Ni-combustion reactor run at 1,100 °C. The water generated by oxidation was removed by a naphion tubing in a dry He stream and a P_4O_{10} water trap. The CH_4-derived CO_2 peak was cryofocussed again. Controlled warming of the trap injected the gas into a continuous flow of He to the mass spectrometer and provided an optimized peak width. The volume of the injected samples was chosen based on the CH_4 concentration measured aboard to allow constant mass injections (e.g., less gas was injected of a sample of high CH_4 concentration). The overall reproducibility of stable carbon isotope determination was 0.6 ‰ for all samples. All isotope ratios are given in δ-notation versus Vienna Pee Dee Belemnite (VPDB) standard.

Current measurements were obtained by an upward-looking ADCP (RD-Instruments, 75 kHz) attached to a lander device that was deployed autonomously at the seafloor. The ADCP covered a depth range of 1,863–1,423 m water depth and was located at 9°07.00′N/84°50.49′W, close to the headwall of the scar in the northwest corner (Fig. 2). The ADCP was deployed from October 16 to 18, 2005. Data were recorded using a BIN size of 10 m and an average ensemble interval of 10 min.

Detailed seafloor video information in the vicinity of the main vent area, which was previously determined by information on the water column CH_4 distribution and video information from towed instruments, was gathered during dives 73 and 74 of ROV Quest (MARUM Bremen) in September 2005 (Brueckmann et al. 2009). This information was used for quantitative assessment of the prevailing vent fauna. Video material recorded in broadcast quality (camera: Insite Atlas 3CCD installed 20 cm above the ROV base) was analyzed in order to estimate the relative coverage of different types of vent-specific fauna at the sea floor, in particular *Beggiatoa*, vesicomyid clams, bathymodiolid mussels, Vestimentifera, and Serpulida. For this task, a transparent slide with a 4 × 5 box raster (where each box counts 5 %) was fixed to the monitor to render more precisely the estimation of the faunal distribution relative to the imaged sea floor. Each of the consecutive freeze images was analyzed along each of the tracks. Similar percentage of closely located positions were summarized and assigned to one category of coverage. Accurate positioning and navigation of the ROV with an accuracy of two meter was achieved by using an ultra-short baseline positioning system (IXSEA GAPS). Processing of ROV navigation data eliminated a number of outliers, which possibly resulted from inaccurate measurements, reflections at boundary layers of different water bodies, or bottom structures (for details, see Schleicher 2006).

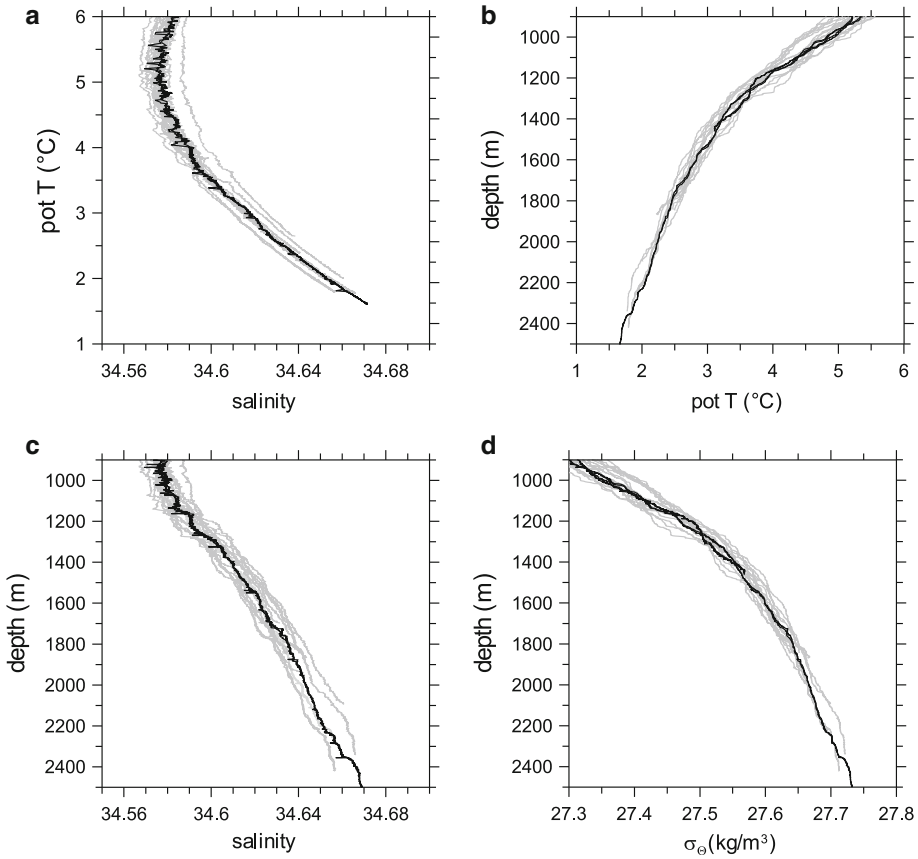

Fig. 3 **a** Potential temperature–salinity graph, profiles of **b** potential temperature, **c** salinity, and **d** potential density (σ_θ) versus depth at stations at Jaco Scar (*gray*) and at reference stations (*black*)

Results

Hydrography

Depth profiles of potential temperature, salinity, and density show that the CH_4 at Jaco Scar is emitted in a well-stratified water mass that is not restricted to the scar. This implies a dominant horizontal spreading of CH_4 from the source to water outside of the scar. Jaco Scar is located at 1,000–2,400 m water depth. At this depth, the eastern part of the Pacific is composed of low-saline Pacific intermediate water (PIW, salinity ca. 34.5) from ~600 to 1,200 m water depth and of Pacific deep water (PDW, salinity: 34.6–34.65 and temperature ~2 °C) filling the basin below (Badan-Dagon 1998). The potential temperature–salinity graph shows a notable influence of low-salinity PIW above ca. 1,500 m (at ~3 °C) whereas water below follows a straight line indicating mixing of two water masses, that is, PIW and PDW (Fig. 3a). Depth profiles of potential temperature, salinity, and potential density from inside the scar are consistent with profiles from reference stations outside the scar (Fig. 3). Multiple profiles indicate the range of the lateral variability within the scar, but also demonstrate that the general vertical structure is undisturbed within the depression formed by the scar. No temperature or salinity anomalies were found near the seep site. Potential temperature decreases gradually from 5 to 2 °C with depth. Salinity increases slightly from 34.58 to 34.67 and potential density (σ_θ) increases from 27.33 to 27.71 kg m^{-3} with water depth. Even though the potential temperature and density profiles show a smaller depth-dependence below 27.58 kg m^{-3} (corresponding to ~1,500 m), density still increases steadily ensuring a well-stratified water column (Fig. 3d).

A 48-h ADCP deployment in 2005 (for location see Fig. 2) indicates that the current pattern within Jaco Scar varies with depth (Fig. 4). The measurements show decreasing current velocities and a general change in direction from northward above ~1,700 m water depth to southward near the seafloor. The mean current velocity (time frame of four tidal cycles) was 52 ± 29 mm s^{-1} at 1,500 m water depth, 44 ± 24 mm s^{-1} at 1,600 m water depth, and 35 ± 19 mm s^{-1} at 1,700 and 1,800 m water depth. At 1,500 m and above, water flowed toward northwest with highest velocities occurring during low tide. The flow turned toward the northeast during high tide and returned clockwise (southerly directions) to the northwest again at low tide. The progress of water toward north/northwest prevailed to about 1,700 m, but the flow showed increased turbulence with incessantly changing directions.

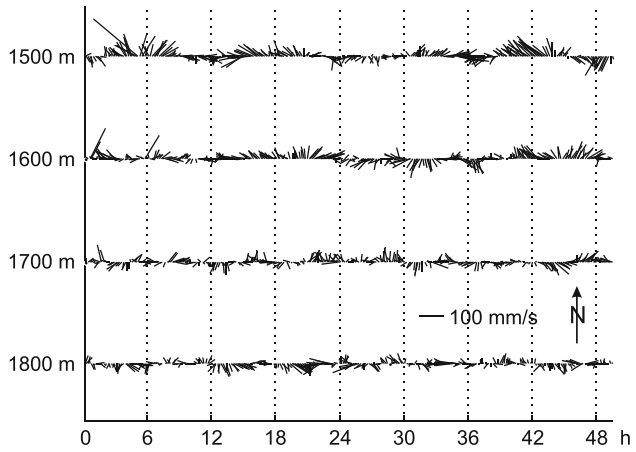

Fig. 4 Stickplot of currents between 1,500 and 1,800 m water depth recorded by ADCP in the northwest corner of Jaco Scar (Fig. 2) over four tidal cycles. Start 16.10.2005 8:10, end 18.10.2005 9:30 (UTC). The current velocity is given by the length of the sticks (see 100 mm s^{-1} scale bar), which point in the direction of the observed current

A tidal cycle could hardly be distinguished. At 1,800 m water depth, the current record indicates a predominant southward flow that only occasionally turned toward the north. The increased turbulence with depth and southerly flow results most likely from the topography of Jaco Scar affecting the general flow toward northwest.

CH_4 concentration

The water column in the area of Jaco Scar was sampled intensively during April/May 2002 (SO163/2) and August/September 2002 (M54/2&3). Two stations, one in the northwest corner and the other at the eastern rim of the scar, were sampled during these two campaigns and again in September 2003 (SO173/3&4) and October 2005 (M66/2) to record temporal variability.

Highest CH_4 concentrations were observed in the density range 27.58–27.68 kg m^{-3} (in 1,500–2,000 m water depth) during all sampling campaigns (Figs. 5a, b, 6) forming a distinct plume, that is, water with CH_4 concentrations above the regional background and an isotopic signature which indicates seepage. The average CH_4 concentration of the 2002 data in this zone was 85.1 nmol L^{-1} ($n = 146$). CH_4 concentrations decreased above this plume (1,000–1,500 m, average 2.0 nmol L^{-1}, $n = 43$) as well as below (2,000–2,400 m, average 7.1 nmol L^{-1}, $n = 18$). However, most values were higher than background values measured at reference stations outside the scar. The average background CH_4 concentration was 1.9 nmol L^{-1} at a station above the scar (R1 in Fig. 1, $n = 5$), and 1.3 nmol L^{-1} and 0.8 nmol L^{-1} at reference stations R2 and R3, respectively, which are located farther away (R2/R3 in Fig. 1, $n = 5/6$).

CH_4 concentrations also differed horizontally (Fig. 5a). Highest values were observed at the northwest corner of the scar, on the western slope of a small ridge (box 1). Concentrations reached up to 1,506 nmol L^{-1} CH_4 there. Ethane concentrations were negligible (M54/CTD151, M54/VESP-MUC173-1&2), resulting in C_1/C_2 ratios between 4,000 and 6,000. The average CH_4 concentration in box 1 (between 27.58 and 27.68 kg m^{-3}) was 244 nmol L^{-1} ($n = 44$). Concentrations decreased from the northwest corner of the scar in every direction. Box 2 includes all stations surrounding the northwest corner. The average CH_4 concentration in box 2 was 20.3 nmol L^{-1} ($n = 75$) in the plume zone. CH_4 concentrations decreased even further to 5.6 nmol L^{-1} ($n = 27$) toward the southwestern opening of the scar. Below the plume in 2,000–2,400 m water depth, CH_4 concentrations decreased from 10.9 nmol L^{-1} (box 2, $n = 9$) within the scar to 3.2 nmol L^{-1} (box 3, $n = 9$) at its southwestern opening. In contrast, the concentrations above the plume were similar to background concentrations: 2.0 nmol L^{-1} (box 1, $n = 12$), 2.1 nmol L^{-1} (box 2, $n = 22$), and 1.8 nmol L^{-1} (box 3, $n = 3$).

Enhanced CH_4 concentrations were found during all sampling campaigns at the repeatedly sampled sites (Fig. 6). Even though CH_4 concentrations fluctuated considerably with time and space, all samples of maximum CH_4 concentration were collected in the density range of the plume. The maximum CH_4 concentrations ranged from 102 to 283 nmol L^{-1} in the northwest corner and from 25 to 99 nmol L^{-1} at the station at the eastern rim (Fig. 2). Hence, maximum CH_4 concentrations in the plume were at least one order of magnitude above background CH_4 concentrations in spring and fall 2002, fall 2003, and fall 2005.

$\delta^{13}C$ signature of CH_4

The carbon isotopic composition of CH_4 gas samples taken in 2002 and of samples collected in 2003 was determined. The range of values differs slightly with water depth (Fig. 5c, 2002 data). $\delta^{13}C$ values range from −62 to −38 ‰ above the plume (1,000–1,500 m, $n = 32$), from −57 to −27 ‰ within the plume (1,500–2,000 m, $n = 143$), and from −58 to −47 ‰ below the plume (2,000–2,400 m, $n = 16$). Most of the CH_4 is enriched in ^{12}C compared with background values which range between −43 and −39 ‰ (unfortunately only samples of station R2 in Fig. 1 could be analyzed, $n = 5$). These isotopically light values found above, within, and below the plume represent the majority of the data. Isotope ratios enriched in ^{13}C compared with background values were only found within the depth range of the CH_4 plume (M54 in Fig. 5c).

Samples of maximum CH_4 concentration of the time series show similar $\delta^{13}C$ values illustrating a persistent

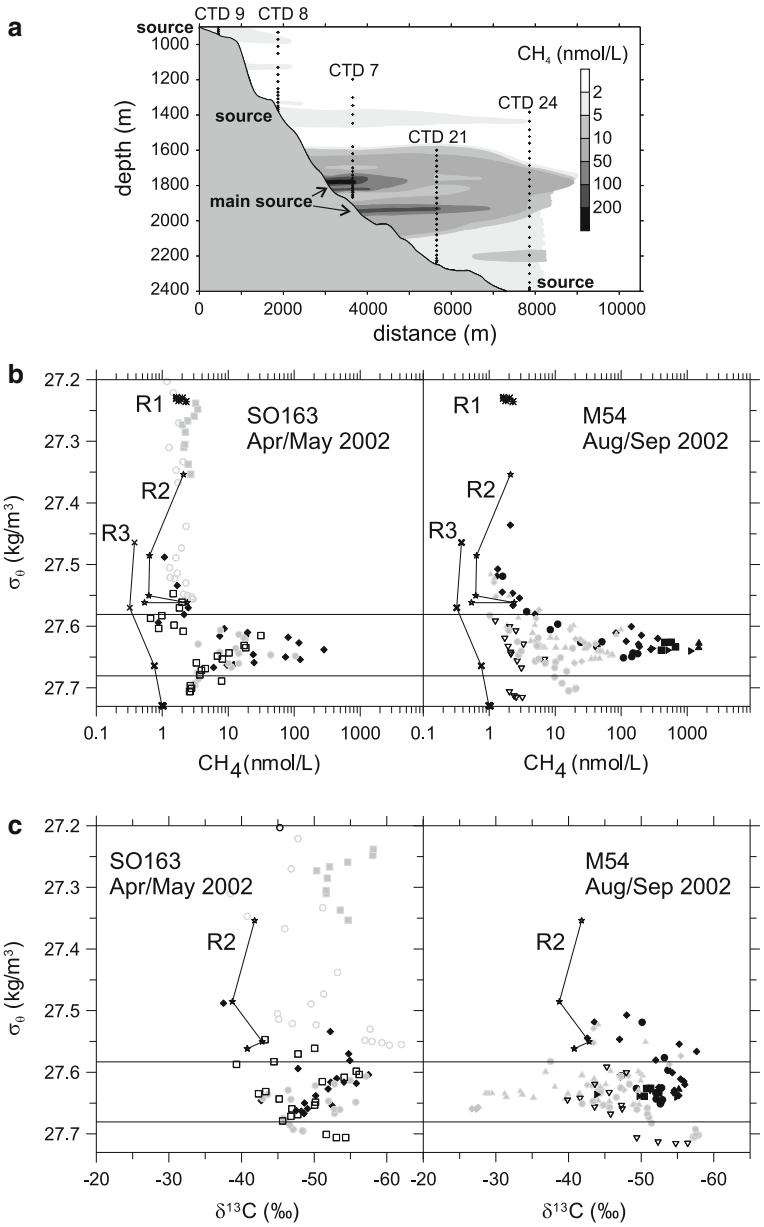

Fig. 5 CH_4 concentration and $\delta^{13}C_{CH_4}$ data. **a** Contour plot of CH_4 concentration along a transect across the slope of Jaco Scar passing close to the main CH_4 source (the transect is shown as *thick*, *dashed line* in Fig. 2), **b** CH_4 concentration and **c** $\delta^{13}C_{CH_4}$ (in ‰ VPDB) versus potential density. *Filled black*, *gray*, and *open symbols* correspond to *box 1*, *box 2*, and *box 3*, respectively. *R1*, *R2*, and *R3* represent samples from corresponding reference stations (for location see Fig. 1). *Horizontal lines* indicate density range of the CH_4 plume

supply of isotopically light CH_4 to the water inside the scar (Fig. 6). Highest CH_4 concentrations in the northwest corner have an isotopic composition of −50 and −53 ‰ in 2002 and a value of −48 ‰ in 2003. Highest CH_4 concentrations sampled at the eastern rim have $\delta^{13}C$ values of −50 ‰ in 2002 and −53 ‰ in 2003.

Biological evidence for CH_4 seepage

Biological evidence for seepage was observed during a video sled survey (M54/OFOS147) which revealed a large field of extremely high abundance of seep-typical vestimentiferan tubeworms (Siboglinidae, Obturata, cf. *Lamellibrachia barhami*) growing on steep sedimentary outcrops in the northwest corner of the scar at depth between 1,750 and 1,850 m. At this particular site, the slide has exposed the lowermost observable stratigraphic units of the hanging wall, suggesting that this is the preferred pathway of CH_4-rich fluids. Vent-indicative clams and mussels were also abundant at the less steep base of the hanging wall and the talus field below. The investigation showed focused fluid seepage from the outcrops, but not from the slide mass. A video-guided VESP-MUC in addition to the CTD/rosette was used for sampling in the vicinity to the field of vestimentifera. The CH_4 concentrations of these samples reach up to 1,506 nmol L^{-1} (M54/VESP-MUC173-2) and are the highest values reported up to date in the water column of nine investigated seep areas along the Costa Rican subduction zone (Bohrmann et al. 2002; Mau et al. 2006).

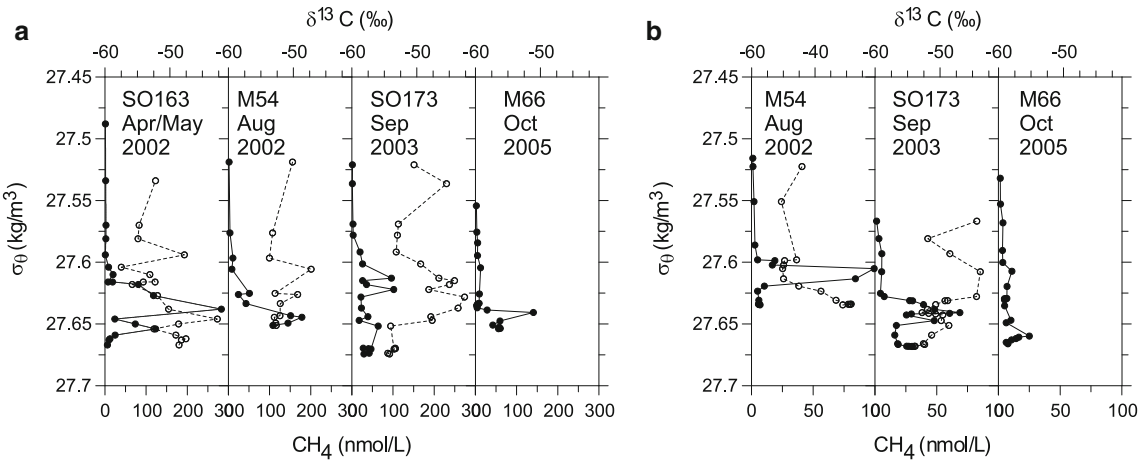

Fig. 6 Time variability at **a** a station in the northwest corner of Jaco Scar and **b** at a station at the eastern rim of the scar (for location see Fig. 2) shown as water column potential density profiles of CH_4 concentration (*filled circles*) and $\delta^{13}C_{CH_4}$ (*open circles*, in ‰ VPDB). Note the different $\delta^{13}C_{CH_4}$ scale in **b** for M54 Aug 2002

Based on these pilot studies, a ROV survey in 2005 was used to collect data for a detailed distribution map and quantitative assessment of the vent-associated fauna in the area (Fig. 7, Supplementary Material Fig. 1). Video analysis confirms a clear zonation of vent-specific fauna, with vestimentiferan tubeworms dominating the areas of highest CH_4 flux on steep and hard grounds, sometimes covering the entire seafloor (Fig. 7, pictures 6, 8, 9). Toward the northwest, some individual areas covered by different forms of vent fauna were observed, which became less abundant with distance from the main vent field (Fig. 7, pictures 1–5).

Discussion

CH_4 distribution

Increased CH_4 concentrations at Jaco Scar indicate a supply of CH_4 from within the scar. Background CH_4 concentrations measured above the scar and at reference sites offshore Costa Rica ranged between 0.3 and 2.4 nmol L^{-1}. The majority of the measurements at the scar, however, showed higher values (Fig. 5a, b). Particularly high CH_4 concentrations were found in the density range between 27.58 and 27.68 kg m^{-3}. Within this density range, the highest CH_4 concentrations were observed in the northwest corner of the scar pointing to a source in this region.

We suggest that CH_4 is emitted dissolved in fluids drained from the seafloor rather than as gas bubbles. Acoustic or video-guided instruments at Jaco Scar during cruise M54/2&3 in 2002 (Weinrebe and Flueh 2002; Soeding et al. 2003) and during cruise M66/2 in 2006 (Brueckmann et al. 2009) support this suggestion, as no gaseous CH_4 was detected during those surveys. In particular, ROV-based investigation of the main vent field in 2005 showed no signs of gas bubbles, neither by video observation nor by forward-looking sonar, an instrument usually very sensitive to gas bubbles (Nikolovska et al. 2008). Also manned diving campaigns using the submersible *Alvin* in 2009/2010 (Levin et al. 2012) provide proof for methane-rich fluid rather than bubble emission. Measured CH_4 concentration profiles show a broad plume in a well-defined density range (Fig. 5a, b). In contrast, capture of CH_4 bubbles during tripping of Niskin bottles would result in a CH_4 profile with sudden concentration peaks at different densities (Grant and Whiticar 2002; Heeschen et al. 2005).

CH_4 spreads horizontally from the source in the northwest corner throughout the scar. Current measurements indicate incessantly changing bottom-water directions, distributing the CH_4 in every direction from the source (Fig. 4). The plume is clearly visible within box 2 and reaches as far as station M54/CTD152 (Fig. 2). Though the current meter data (Fig. 4) suggest enhanced turbulence in the deeper layers, the CH_4-enriched waters mostly spread along isopycnal surfaces.

Due to the open morphology of the scar, a homogeneous horizontal distribution of CH_4 was not observed. Background water is constantly flowing into the scar and mixes with the CH_4-rich water as confirmed by $\delta^{13}C$ values that indicate mixing processes throughout the water column (see "Fate of CH_4 in the water column" section).

CH_4 source

CH_4 seepage in the northwest corner of the scar is indicated by the occurrence of dense biological communities (Fig. 7)

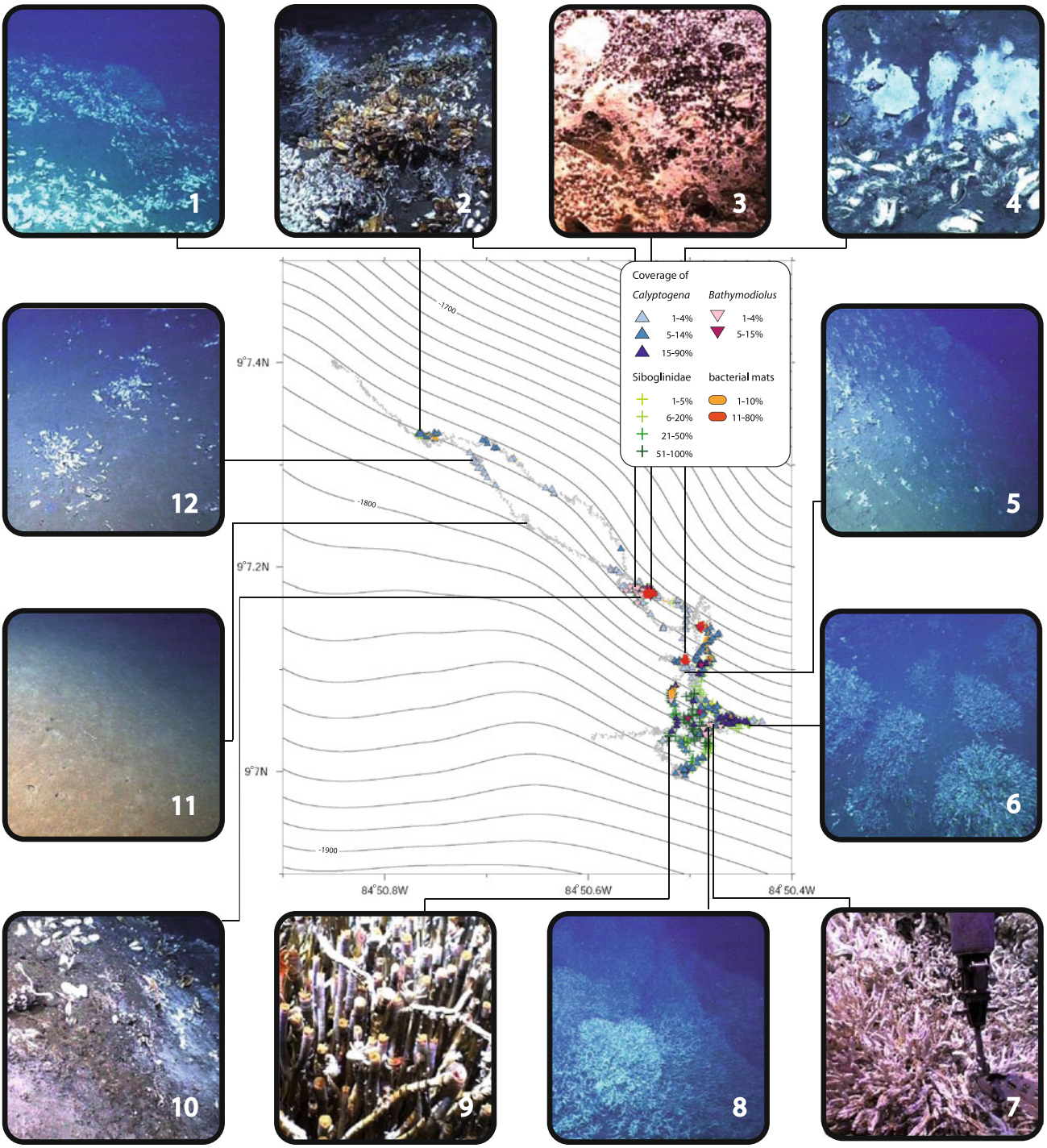

Fig. 7 Distribution of chemosynthetic communities in the northwest corner of Jaco Scar. The section displayed in the map corresponds approximately to the *box 1* in Fig. 2. The percent seafloor coverage by the major groups is shown along the ROV dive track; separate maps for each group are depicted in the Supplementary Material Figure 1. Subfigures *1–12* are video frame grabs illustrating seep-specific organisms and the seafloor characteristics. *1* vesicomyid clams and two bushes of vestimentiferan tubeworms, *2* bathymodiolin mussels attached to authigenic carbonates, vesicomyid clams, vestimentifera, *3 thick*, *colored* microbial mats, *4* vesicomyid clams and white microbial mats, *5* serpulida (polychaeta) attached to hard substrate, *6* bushes of vestimentifera, *7* dense aggregates of serpulida, *8* vestimentifera and serpulida, *9* vestimentifera, *10* vesicomyid and bathymodiolin mussels, white microbial mat, *11* plain sediment, *12* cluster of vesicomyid clams. Photos by MARUM, Bremen, Germany

that are typically found at seeps (Sibuet and Olu 1998). Most of the observed taxonomic groups (vestimentiferan tubeworms, mytilid, and vesicomyid bivalves) have been shown to entirely depend on chemosynthesis (Fisher 1990). The observed microbial mats consist of filamentous sulfur-oxidizing bacteria of the genus *Beggiatoa* which also commonly occur at seep sites (Sahling et al. 2002). Dense aggregations of Serpulida have been reported from other seeps (Olu et al. 1996b; Torres et al. 1996). However, although Serpulida appear seep dependant, their ecological functioning is not well known. The observed dense biological community found in the northwest corner suggests that CH_4 seepage within the scar is focused at this particular site. This hypothesis is supported by the measurement of the highest CH_4 concentrations in this area, close to the vestimentiferan tubeworm colonies and by direct *Alvin*-observations (Levin et al. 2012).

The δ^{13}C-values of CH_4 samples close to the source show values of −50 to −55 ‰. These values are right between critical values described in the literature classifying microbial and thermogenic CH_4 in sediments. Whiticar (1996, 1999) reported C isotope ratios of microbial CH_4 varying in $\delta^{13}C_{CH_4}$ between −100 and −50 ‰, whereas Bernard et al. (1977) and Paull et al. (2000) stated values between −90 and −55 ‰. In comparison, thermogenic CH_4, which is enriched in ^{13}C, has $\delta^{13}C_{CH_4}$ values ranging from −50 ‰ to −20 ‰ as described by Whiticar (1990, 1999) or values more positive than −55 ‰ as stated by Bernard et al. (1977) and Paull et al. (2000). The C_1/C_2 ratio is another way to distinguish between microbial and thermogenic origin of CH_4. A methane/ethane ratio of >1,000 is typically for microbial CH_4, whereas a ratio of less than 100 is characteristic of thermogenic CH_4 (Bernard et al. 1977; Paull et al. 2000). Although this division is based on sedimentary data, it is commonly applied for water samples (Faber et al. 1996; Faure et al. 2010; Schneider von Deimling et al. 2011). At Jaco Scar, sampling of sediments proved to be difficult due to steep slopes. Therefore, we used water column samples that were taken within 2–3 m range to the main source (M54/CTD151, M54/VESP-MUC173-1&2). The C_1/C_2 ratio of these samples might already be modified by mixing with ocean water and hydrocarbon oxidation. However, the measured C_1/C_2 ratios range between 4,000 and 6,000 and are one order of magnitude higher than values that indicate a thermogenic origin. These ratios agree with ratios found in core samples drilled during ODP Leg 170 about 100 km distant from Jaco Scar (Lückge et al. 2002). $\delta^{13}C_{CH_4}$ values and $C_1/(C_2 + C_3)$ ratios measured in these cores suggest a mixture of microbial CH_4 with 0.03–1.8 % thermogenic CH_4. However, $\delta^{13}C_{CH_4}$ values in the ODP core samples range from −82 to −61 ‰. If CH_4 at Jaco Scar and in the ODP cores were of the same origin, a significant part of the gas must have been already oxidized before emission from the sediment outcrop at Jaco Scar. However, the contribution of thermogenic CH_4 is possibly higher at Jaco Scar. Recent results show that Jaco Scar is a very special case, an intermediate between a hydrothermal vent and a cold seep (Levin et al. 2012). Shimmering water with temperatures up to 3 °C warmer than ambient water was observed during *Alvin* dives. These observations and preferable oxidation of higher hydrocarbons in sediments as suggested by Joye et al. (2004) and Niemann et al. (2006) indicate that a significant portion of the CH_4 emitted at Jaco Scar might be of thermogenic origin. Based on our results and the new findings about this structure, CH_4 within Jaco Scar originates most likely from a mixture of microbial or thermogenic sources, but the relative importance of the two origins cannot be inferred from our data.

Samples with δ^{13}C-values below −55 ‰ (CH_4 enriched in ^{12}C) were found at four other stations indicating the existence of additional sources in the scar. The source in the northwest corner releases CH_4 into the water column with densities between 27.63 and 27.64 kg m^{-3}, whereas the samples with lighter isotopic composition were collected at densities above and below (SO163/CTD07, SO163/CTD08, M54/CTD180, and M54/CTD47, see Supplementary Material Table 1). Taking the variation in potential density data of ∼±0.03 kg m^{-3} into account and considering that CH_4 is dominantly distributed along isopycnals (Fig. 3d), additional CH_4-sources apparently exist in the density range 27.55–27.56 kg m^{-3} (SO163/CTD08) and 27.69–27.7 kg m^{-3} (M54/CTD180). That is, additional CH_4 is emitted into the water column above and below the plume. However, these sources are minor with respect to the main source in the northwest corner of the scar, as these samples have CH_4 concentrations of less than 21 nmol L^{-1}.

Fate of CH_4 in the water column

After injection of CH_4 into the water column, its concentration decreases with distance from the seep. This can be caused by mixing and/or aerobic oxidation. The stable carbon isotope ratio of CH_4 indicates that both processes take place.

Roughly half of the data (122 of 232 samples) can be attributed to mixing processes. Mixing is commonly shown as a straight line in a δ^{13}C versus 1/CH_4 plot (Keeling 1958, 1961; Faure 1986; Tsunogai et al. 2000). Figure 8 shows such a plot and illustrates the range of mixing with the solid line representing the limit of values that can be explained solely by mixing. The solid line illustrates mixing of seep-CH_4 from the source in the northwest corner of the scar and the highest background CH_4

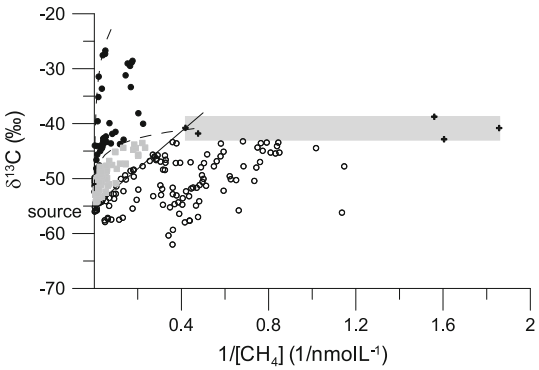

Fig. 8 $\delta^{13}C_{CH_4}$ versus $1/CH_4$. The *solid line* represents mixing of the most CH_4-enriched samples near the main source with background water, *dashed lines* indicate oxidation trends based on fractionation factors (α) between 1.005 and 1.016, "source" stands for seepage in the northwest corner of Jaco Scar, and the *gray-shaded rectangle* includes background data measured at station *R2* in Fig. 1. *Circles* show mixing between source and background water, *gray squares* indicate mixing and oxidation of CH_4, *filled circles* follow the oxidation trends

concentration. Background samples were collected at reference site R2 and lie within the area highlighted by the gray-shaded rectangle in Fig. 8. Some values that plot below the mixing line might be attributed to mixing of ^{12}C-enriched CH_4 emitted from smaller sources above and below the main plume and background water.

The other half of the CH_4 isotopic data (110 of 232 samples) cannot be explained by mixing alone, showing slight to strong enrichment of ^{13}C. Oxidation of CH_4 causes a depletion in ^{12}C and, hence, an enrichment of ^{13}C in the remaining CH_4 pool (Whiticar and Faber 1986). For these ^{13}C-enriched samples, oxidation trends were calculated using the Rayleigh fractionation after Coleman et al. (1981) from values measured at the source in the northwest corner (1,506 nmol L^{-1}/−55 ‰) and fractionation factors (α) between 1.005 and 1.016. All chosen α represent the lower end of published values ranging between $\alpha = 1.005$ and 1.031 (Barker and Fritz 1981; Whiticar and Faber 1986; Happell et al. 1994; Grant and Whiticar 2002). The calculated oxidation trends are shown in Fig. 8, which also point out that lower α fit more data than the highest α chosen. The small fractionation factors and the 62 samples lying between the mixing trend of source and background CH_4 and the oxidation trend calculated from $\alpha = 1.005$ indicate that only a fraction of the CH_4 observed in the scar was microbially oxidized. We speculate that the remainder will be oxidized further during transport within the scar and out of the scar.

Temporal variability

Two sites were repeatedly sampled in order to observe the persistence of seepage of CH_4-rich fluids. The northwest corner was sampled twice in 2002, once in 2003, and again in 2005. A station at the eastern slope was sampled once in 2002, in 2003, and in 2005 (Fig. 6). Even though the internal structures of the observed plumes (CH_4 concentration and depth/density of CH_4 maxima, Fig. 6) fluctuate with space and time, CH_4 concentrations are elevated compared with background concentrations (1.9–0.8 nmol L^{-1}) at all times of sampling at both sites. This indicates that CH_4 is added to the water column regularly. Bohrmann et al. (2002) reported on high CH_4 concentrations at Jaco Scar at the same station in the northwest corner based on data of 1999. Therefore, CH_4-rich fluids appear to discharge repeatedly from the outcrop at Jaco Scar over at least 6 years. Whether the discharge of CH_4 is continuous or intermittent cannot be inferred from the data, but a possible link to earthquake activity was discussed in Mau et al. (2007) for this slide as well as for three CH_4-discharging mud extrusions. A strong decrease in CH_4 concentrations from one year to the next at sites up to 300 km apart could not be explained by current or tidal variations. Thus, the authors suggest that a large earthquake prior to the first survey might have induced an increase in CH_4 discharge at the investigated seep sites, which was not observed during the second survey. The CH_4 seems to have a similar origin, because the isotope ratios of CH_4 of the concentration maxima vary only slightly.

Comparison with other seep sites

Seepage activity has also been observed at other scars offshore Costa Rica and along the Aleutian subduction zone. Suess et al. (1998) detected a CH_4 content of 7 nmol L^{-1} at a scar along the Aleutian subduction zone, which is situated in 5,000 m water depth. At Parrita Scar situated at the Costa Rican margin (Fig. 1), the maximum CH_4 concentration did not exceed 20 nmol L^{-1} (Soeding et al. 2003). Therefore, in both cases, analyses showed considerably lower CH_4 concentrations. However, only detailed sampling can verify seepage within >50 km^2 areas. At the scar at the Aleutian subduction zone, two hydrocasts were sampled and at Parrita Scar only one. By chance, these sampling stations may have been too far away from a source or upstream of a source. Hence, these reported lower concentrations compared with Jaco Scar at these two structures could be due to low-resolution sampling.

In addition, CH_4 concentrations at Jaco Scar were compared with those of different seep sites such as hydrothermal active areas, mud extrusions, or other cold seep sites (Table 1). For this purpose, the maximum CH_4 concentration as well as the average excess CH_4 concentration was used. The latter was obtained by averaging CH_4 concentrations at the seep sites and subtracting the regional background CH_4 contribution. As indicated in Table 1, the

Table 1 Maximum CH_4 concentration, average excess CH_4 concentration, and CH_4 output of different seep sites associated with different geological structures

Area	Seep type	Max. CH_4 concentration (nmol L^{-1})	Excess CH_4 concentration (nmol L^{-1})	Output (10^6 mol $year^{-1}$)	References
Jaco Scar off Costa Rica	Fluid seepage	1,506	15.9	–	This study
Izena Cauldron, Okinawa Trough	Hydrothermal venting	706	61.6	1.1	Watanabe et al. (1995)
Myojin Knoll Caldera, Izu-Bonin Arc	Hydrothermal venting	11	3.2	0.03–0.13	Tsunogai et al. (2000)
Mound Culebra off Costa Rica	Fluid seepage	42	7.8	0.6	Mau et al. (2006)
Mound 10 off Costa Rica	Fluid seepage	19	–	–	Mau et al. (2006)
Mound 12 off Costa Rica	Fluid seepage	107	11.4	0.4	Mau et al. (2006)
Mound 11 off Costa Rica	Fluid seepage	17	2.8	0.07	Mau et al. (2006)
Håkon Mosby Mud Volcano, Norwegian Sea	Gas emission and fluid seepage	$>10^4$	–	2.5–11.3	Sauter et al. (2006)
				14	Felden et al. (2010)
Northern summit, Hydrate Ridge off Oregon	Gas emission and fluid seepage	4,400	7.3	4.7	Heeschen et al. (2005)
Southern summit, Hydrate Ridge off Oregon	Gas emission and fluid seepage	1,400	19.8	3.5	Heeschen et al. (2005)
Tommeliten, North Sea	Gas ebullition	268	–	1.5	Schneider von Deimling et al. (2011)
Hikurangi Margin, New Zealand	Gas emission and fluid seepage	90–3,500	–	–	Faure et al. (2010)

maximum CH_4 concentration found at Jaco Scar is higher than maximum values observed at hydrothermal areas and mud extrusions offshore Costa Rica. Maximum CH_4 concentration at Jaco Scar even reach values measured at Hydrate Ridge, a very active seep area (Heeschen et al. 2005) and the Tommeliten area in the North Sea (Schneider von Deimling et al. 2011). Better and more reliable results can be obtained by comparison of the average excess CH_4 concentration at different seep sites. In general, excess CH_4 concentration at Jaco Scar is at the upper end of values observed for the other structures. In comparison with mud extrusions at the Costa Rican margin, it is even higher. A lower concentration is only observed in comparison with the Izena Cauldron at the east side of the Okinawa Trough (Watanabe et al. 1995) and at the southern summit of Hydrate Ridge (Heeschen et al. 2005). Most likely, the excess CH_4 concentration at Håkon Mosby mud volcano is also higher than the concentration at Jaco Scar (data not available in Sauter et al. 2006; Felden et al. 2010). In summary, CH_4 output at Jaco Scar appears to be as significant as output from these other natural CH_4 sources in the ocean (Table 1).

Conclusions

Jaco Scar is one of the scars along the Pacific coast offshore Costa Rica that formed by seamount subduction. Detailed investigations of the CH_4 concentrations inside this structure, CH_4 carbon stable isotopic signature, and the occurrence of chemosynthetic communities revealed a major discharge area in the northwest corner of the scar. Besides, additional point sources supplying CH_4 at lower concentrations in density layers above and below the main CH_4 plume were found. The isotope ratio of the discharging CH_4 and recent findings (Levin et al. 2012) suggest partial microbial and thermogenic origin of the gas. CH_4 is distributed and mixed along isopycnals within the area of the scar and oxidized in the center of the main plume.

Scars or slides are common features along continental margins (Etnoyer et al. 2010; Staudigel and Clague 2010); however, little is known about their role in the CH_4 cycle. A comparison of excess CH_4 concentration with hydrothermal active areas and various cold seep sites illustrates that CH_4 output of scars might be of similar significance. A persistent supply of CH_4 to the water was observed for a time span of 6 years, suggesting that as long as the scar remains in an approximately similar geological setting as presently, that is, in a mid slope position, CH_4 is recurrently transferred to deep waters. Whether Jaco Scar is an exception caused by the simultaneous emission of hydrothermal and cold seep fluids (Levin et al. 2012) or whether scars/slides in general are another but so far neglected source of CH_4 to the ocean needs to be clarified. Further scrutinizing of the global abundance of scars from

bathymetric information as well as more detailed investigations of CH_4 seepage from representative scars is required to identify their role in the CH_4 budget of the ocean.

Acknowledgments Many thanks to the scientists, masters, and crews aboard research vessels SONNE and METEOR during cruises SO 163, M 54, SO 173, and M66 for their support, information, and discussion. We are grateful for the many helpful hands during sampling, most of all Karen Stange and Bert Mantzke. Karen Stange provided also shore-based stable carbon isotope analysis. For comments and discussion, we like to thank Robin Keir, Jürgen Gossler, Christian Hensen, Warner Brückmann, Steffen Kutterrolf, Roger Luff, Oliver Bartdorff, and Heidi Wehrmann. This publication is contribution no. 80 of the Sonderforschungsbereich 574 "Volatiles and Fluids in Subduction Zones" at the University of Kiel.

References

Badan-Dagon A (1998) Coastal circulation from the Galapagos to the Gulf of California. In: Robinson AR, Brink KH (eds) The sea, vol 11: the global coastal ocean—regional studies and syntheses. Wiley, Hoboken, NJ, pp 315–343

Ballance PF, Scholl DW, Vallier TL, Herzer RH (1989) Subduction of a late cretaceous seamount of the Loisville Ridge at the Tonga Trench: a model of normal and accelerated tectonic erosion. Tectonics 8:953–962

Barker JF, Fritz P (1981) Carbon isotope fractionation during microbial methane oxidation. Nature 293:289–291

Bernard BB, Brooks JM, Sackett WM (1977) A geochemical model for the characterization of hydrocarbon gas sources in marine sediments. In: Proceedings of offshore technology conference, pp 435–438

Bohrmann G, Jung C, Heeschen K, Weinrebe W, Baranov B, Cailleau B, Heath R, Hühnerbach V, Hort M, Masson D, Schaffer I (2002) Widespread fluid expulsion along the seafloor of Costa Rica convergent margin. Terra Nova 14:69–79

Brueckmann W, Rhein M, Rehder G, Bialas J, Kopf A (2009) SUBFLUX, Cruise No. 66, August 12–December 22, 2005. METEOR-Berichte 09-2. Universitaet Hamburg, Hamburg

Cita MB, Woodside JM, Ivanov MK, Kidd RB, Limonov AF, Scientific Staff of Cruise TTR3-Leg2 (1995) Fluid venting from a mud volcano in the Mediterranean Ridge diapiric belt. Terra Nova 7:453–458

Clark J, Washburn L, Hornafius JS, Luyendyk BP (2000) Dissolved hydrocarbon flux from natural marine seeps to the southern California Bight. J Geophys Res 105:11509–11522

Coleman DD, Risatti JB, Schoell M (1981) Fractionation of carbon and hydrogen isotopes by methane-oxidizing bacteria. Geochim Cosmochim Acta 45:1033–1037

Collot J-Y, Fisher MA (1989) Formation of forearc basins by collision between seamounts and accretionary wedges: an example from the New Hebrides subduction zone. Geology 17:930–933

Cranston RE, Ginsburg GD, Soloviev VA, Lorenson TD (1994) Gas venting and hydrate deposits in the Okhotsk Sea. Bull Geol Soc Den 41:80–85

Damm E, Budeus G (2003) Fate of vent-derived methane in seawater above the Håkon Mosby mud volcano (Norwegian Sea). Mar Chem 82:1–11

Dia AN, Aquilina L, Boulègue J, Bourgois J, Suess E, Torres M (1993) Origin of fluids and related barite deposits at the vent sites along the Peru convergent margin. Geology 21:1099–1102

Etnoyer PJ, Wood J, Shirley TC (2010) How large is the seamount biome? Oceanography 23:206–209

Faber E, Berner U, Gerling P, Hollerbach A, Stahl WJ, Schroeder HG (1996) Isotopic tracing of methane in water and exchange with the atmosphere. Energy Convers Manag 37:1193–1198

Faure G (1986) Principles of isotope geology. Wiley, New York

Faure K, Greinert J, Schneider von Deimling J, McGinnis DF, Kipfer R, Linke P (2010) Methane seepage along the Hikurangi margin of New Zealand: geochemical and physical data from the water column, sea surface and atmosphere. Mar Geol 272:170–188

Felden J, Wenzhöfer F, Feseker T, Boetius A (2010) Transport and consumption of oxygen and methane in different habitats of the Håkon Mosby mud volcano (HMMV). Limnol Oceanogr 55:2366–2380

Fisher CR (1990) Chemoautotrophic and methanotrophic symbioses in marine invertebrates. Aquat Sci 2:399–436

Ginsburg GD, Milkov AV, Soloviev VA, Egorov AV, Cherkashev GA, Vogt PR, Crane K, Lorenson TD, Khutorskoy MD (1999) Gas hydrate accumulation at the Håkon Mosby mud volcano. Geo-Mar Lett 19:57–67

Grant NJ, Whiticar MJ (2002) Stable carbon isotopic evidence for methane oxidation in plumes above Hydrate Ridge, Cascadia Oregon Margin. Global Biogeochem Cycles 16(4):71-1–71-13

Grasshoff K, Ehrhardt M, Kremling K (1997) Methods of seawater analysis. Verlag Chemie, Gulf Publishing, Houston

Haese RR, Meile C, van Cappellen P, de Lange GJ (2003) Carbon geochemistry of cold seeps: methane fluxes and transformation in sediments from Kazan mud volcano, eastern Mediterranean Sea. Earth Planet Sci Lett 212:361–375

Happell JD, Chanton JP, Showers WS (1994) The influence of methane oxidation on the stable isotopic composition of methane emitted from Florida swamp forests. Geochim Cosmochim Acta 58:4377–4388

Harders R, Ranero C, Weinrebe W, Behrmann JH (2011) Submarine slope failure along the convergent continental margin of the Middle American Trench. Geochem Geophys Geosyst 12:1–26

Heeschen KU, Collier RW, de Angelis MA, Linke P, Suess E, Klinkhammer GP (2005) Methane sources, distributions, and fluxes from cold vent sites at Hydrate Ridge, Cascadia Margin. Global Biogeochem Cycles 19:GB2016

Henry P, Le Pichon X, Lallement S, Lance S, Martin JB, Foucher J-P, Fiala-Medioni A, Rostek F, Guilhaumou N, Pranal V, Castrec M (1996) Fluid flow in and around a mud volcano field seaward of the Barbados accretionary wedge: results from Manon cruise. J Geophys Res 101:20297–20323

Hornafius JS, Quigley DC, Luyendyk BP (1999) The world's most spectacular marine hydrocarbon seeps (Coal Oil Point, Santa Barbara Channel, California): quantification of emission. J Geophys Res 104:20703–20711

Hovland M, Gallagher JW, Clennell MB, Lekvam K (1997) Gas hydrate and free gas volumes in marine sediments: example from the Niger Delta front. Mar Pet Geol 14:245–255

Hühnerbach V, Masson DG, Bohrmann G, Bull JM, Weinrebe W (2005) Deformation and submarine landsliding caused by seamount subduction beneath the Costa Rican continental margin—new insights from high-resolution sidescan sonar data. Geological Society spec. publ, London

Joye SB, Boetius A, Orcutt BN, Montoya JP, Schulz HN, Erickson MJ, Lugo SK (2004) The anaerobic oxidation of methane and sulfate reduction in sediments from Gulf of Mexica cold seeps. Chem Geol 205:219–238

Judd A, Hovland M (2007) Seabed fluid flow. Cambridge University Press, Cambridge

Judd AG, Davies G, Wilson J, Holmes R, Baron G, Bryden I (1997) Contributions to atmospheric methane by natural seepages on the U.K. continental shelf. Mar Geol 140:427–455

Judd AG, Hovland M, Dimitrov LI, Garcia Gil S, Jukes V (2002) The geological methane budget at continental margins and its influence on climate change. Geofluids 2:109–126

Keeling CD (1958) The concentration and isotopic abundances of atmospheric carbon dioxide in rural areas. Geochim Cosmochim Acta 13:322–334

Keeling CD (1961) The concentration and abundance of carbon dioxid in rural and marine air. Geochim Cosmochim Acta 24:277–298

King C-Y (1986) Gas geochemistry applied to earthquake prediction: an overview. J Geophys Res 91:12269–12281

Kopf A, Behrmann JH (2000) Extrusion dynamics of mud volcanoes on the Mediterranean Ridge accretionary complex. In: Vendeville B, Mart Y, Vigneresse J-L (eds) From the Artic to the Mediterranean: salt, shale, and igneous diapirs in and around Europe. Journal of the Geological Society, Spec. Publ., London, pp 169–204

Kulm LD, Suess E, Moore JC, Carson B, Lewis BT, Ritger SD, Kadko DC, Thornburg TM, Embley RW, Rugh WD, Massoth GJ, Langseth MG, Cochrane GR, Scamman RL (1986) Oregon subduction zone: venting, fauna, and carbonates. Science 231:561–566

Kvenvolden KA, Lorenson TD, Reeburgh WS (2001) Attention turns to naturally occuring methane seepage. EOS 82:457

Lallemand S, Le Pichon X (1987) Coulomb wedge model applied to the subduction of seamounts in the Japan Trench. Geology 15:1065–1069

Lammers S, Suess E (1994) An improved head-space analysis method for methane in seawater. Mar Chem 47:115–125

Lein A, Vogt P, Crane K, Egorov A, Ivanov M (1999) Chemical and isotopic evidence for the nature of the fluid in CH_4-containing sediments of the Håkon Mosby mud volcano. Geo-Mar Lett 19:76–83

Levin AL, Orphan VJ, Rouse GW, Rathburn AE, Ussler W III, Cook GS, Goffredi SK, Perez EM, Waren A, Grupe BM, Chadwick G, Strickrott B (2012) A hydrothermal seep on the Costa Rica margin: middle ground in a continuum of reducing ecosystems. Proc R Soc B. doi:10.1098/rspb.2012.0205

Linke P, Suess E, Torres M, Martens V, Rugh WD, Ziebis W, Kulm LD (1994) In situ measurement of fluid flow from cold seeps at active continental margins. Deep Sea Res Pt I 41:721–739

Lückge A, Kastner M, Littke R, Cramer B (2002) Hydrocarbon gas in the Costa Rica subduction zone: primary composition and post-genetic alteration. Org Geochem 33:933–943

Mau S, Sahling H, Rehder G, Suess E, Linke P, Soeding E (2006) Estimates of methane output from mud extrusions at the erosive convergent margin off Costa Rica. Mar Geol 225:129–144

Mau S, Rehder G, Arroyo IG, Gossler J, Suess E (2007) Indications of a link between seismotectonics and CH_4 release from seeps off Costa Rica. Geochem Geophys Geosyst 8:Q04003. doi: 04010.01029/02006GC001326

Niemann H, Duarte J, Hensen C, Omoregie E, Magalhaes VH, Elvert M, Pinheiro LM, Kopf A, Boetius A (2006) Microbial methane turnover at mud volcanoes of the Gulf of Cadiz. Geochim Cosmochim Acta 70:5336–5355

Nikolovska A, Sahling H, Bohrmann G (2008) Hydroacoustic methodology for detection, localization, and quantification of gas bubbles rising from the seafloor at gas seeps from the Black Sea. Geochem Geophys Geosyst 9. doi:10.1029/2008GC002118

Olu K, Duperret A, Sibuet M, Foucher J-P, Fiala-Medioni A (1996a) Structure and distribution of cold seep communities along the Peruvian active margin: relationship to geological and fluid patterns. Mar Ecol Prog Ser 132:109–125

Olu K, Sibuet M, Harmegnies F, Foucher J-P, Fiala-Medioni A (1996b) Spatial distribution of diverse cold seep communities living on various diapiric structures of the southern Barbados prism. Prog Oceanogr 38:347–376

Paull CK, Lorenson TD, Borowski WS, Ussler W III, Olsen K, Rodriguez NM (2000) Isotopic composition of CH_4, CO_2 species, and sedimentary organic matter within samples from the Blake Ridge: Gas source implications. In: Paull CK, Matsumoto R, Wallace PJ, Dillon WP (eds) Proceedings of the ocean drilling program scientific result. Ocean Drilling Program, College Station, TX, pp 67–78

Ranero CR, von Huene R (2000) Subduction erosion along the Middle America convergent margin. Nature 404:748–752

Reeburgh WS (2007) Oceanic methane biogeochemistry. Chem Rev 107:486–513

Reed DL, Silver EA, Tagudin JE, Shipley TH, Vrolijk P (1990) Relations between mud volcanoes, thrust deformation, slope sedimentation, and gas hydrate, offshore north Panama. Mar Pet Geol 7:44–54

Rehder G, Keir RS, Suess E, Rhein M (1999) Methane in the northern Atlantic controlled by microbial oxidation and atmospheric history. Geophys Res Lett 26:587–590

Sahling H, Rickert D, Lee RW, Linke P, Suess E (2002) Macrofaunal community structure and sulfide flux at gas hydrate deposits from the Cascadia convergent margin, NE Pacific. Mar Ecol Prog Ser 231:121–138

Sahling H, Bohrmann G, Spiess V, Bialas J, Breitzke M, Ivanov M, Kasten S, Krastel S, Schneider R (2008a) Pockmarks in the Northern Congo Fan area, SW Africa: complex seafloor features shaped by fluid flow. Mar Geol 249:206–225

Sahling H, Masson DG, Ranero C, Huehnerbach V, Weinrebe W, Klaucke I, Buerk D, Brueckmann W, Suess E (2008b) Fluid seepage at the continental margin offshore Costa Rica and southern Nicaragua. Geochem Geophys Geosyst 9:1–22

Sahling H, Bohrmann G, Artemov YG, Bahr A, Bruening M, Klapp SA, Klaucke I, Kozlova E, Nikolovska A, Pape T, Reitz A, Wallmann K (2009) Vodyanitskii mud volcano, Sorokin trough, Black Sea: geological characterization and quantification of gas bubble streams. Mar Pet Geol 26:1799–1811

Sauter EJ, Muyakshin SI, Charlou J-L, Schlüter M, Boetius A, Jerosch K, Damm E, Foucher J-P, Klages M (2006) Methane discharge from a deep-sea submarine mud volcano into the upper water column by gas hydrate-coated methane bubbles. Earth Planet Sci Lett 243:354–365

Schleicher T (2006) Bestimmung von ventspezifischen Faunenvergesellschaftungen am mittelamerikanischen Kontinentalrand mit Hilfe quantitativer Videoauswertung. Diploma thesis, Kiel

Schmale O, Beaubien SE, Rehder G, Greinert J, Lombardi S (2010) Gas seepage in the Dnepr paleo-delta area (NW-Black Sea) and its regional impact on the water column methane cycle. J Mar Syst 80:90–100

Schneider von Deimling J, Rehder G, Greinert J, McGinnis DF, Boetius A, Linke P (2011) Quantification of seep-related methane gas emissions at Tommeliten, North Sea. Cont Shelf Res 31:876–878

Sibuet M, Olu K (1998) Biogeography, biodiversity and fluid dependence of deep-sea cold-seep communities at active and passive margins. Deep Sea Res Pt II 45:517–567

Soeding E, Wallmann K, Suess E, Flueh E (2003) RV METEOR Cruise Report M54/2+3 Fluids and Subduction Costa Rica 2002, Kiel

Staudigel H, Clague DA (2010) The geological history of deep-sea volcanoes. Oceanography 23:58–71

Suess E, Bohrmann G, von Huene R, Linke P, Wallmann K, Lammers S, Sahling H, Winckler G, Lutz RA, Orange D (1998) Fluid venting in the eastern Aleutian subduction zone. J Geophys Res 103:2597–2614

Tissot BP, Welte DH (1984) Petroleum formation and occurrence. Springer, Heidelberg

Torres ME, Bohrmann G, Suess E (1996) Authigenic barites and flux of barium associated with fluid seeps in the Peru subduction zone. Earth Planet Sci Lett 144:469–481

Tsunogai U, Yoshida N, Ishibashi J, Gamo T (2000) Carbon isotopic distribution of methane in deep-sea hydrothermal plume, Myojin Knoll Caldera, Izu-Bonin arc: implications for microbial methane oxidation in the oceans and applications to heat flux estimation. Geochim Cosmochim Acta 64:2439–2452

Valentine DL, Blanton DC, Reeburgh WS, Kastner M (2001) Water column methane oxidation adjacent to an area of active hydrate dissociation, Eel River Basin. Geochim Cosmochim Acta 65:2633–2640

von Huene R, Ranero CR, Weinrebe W (2000) Quaternary convergent margin tectonics of Costa Rica, segmentation of the Cocos Plate, and Central American volcanism. Tectonics 19:314–334

von Rad U, Berner U, Delisle G, Doose-Rolinski H, Fecher N, Linke P, Lückge A, Roeser HA, Schmaljohann R, Wiedicke M, Party SS (2000) Gas and fluid venting at the Makran accretionary wedge off Pakistan. Geo Mar Lett 20:10–19

Watanabe S, Tsurushima N, Kusakabe M, Tsunogai S (1995) Methane in Izena Cauldron, Okinawa Trough. J Oceanogr 51:239–255

Weinrebe W, Flueh E (2002) RV Sonne, Cruise Report SO 163, Subduction I, Balboa-Caldera-Balboa (March 13–May 21, 2002). GEOMAR Report 106:534

Whiticar MJ (1990) A geochemical perspective of natural gas and atmospheric methane. 14th EAOG Mtg. Paris, 1989. In: Durand B, Behar F (eds) Advances in organic geochemistry, 1989. Organic Geochemistry, pp 531–547

Whiticar MJ (1996) Isotope tracking of microbial methane formation and oxidation. In: Adams DD, Crill PM, Seitzinger SP (eds) Cycling of reduced gases in the hydrosphere. E. Schweizerbart'sche Verlagsbuchhandlung (Nägele u. Obermiller), Stuttgart, pp 39–54

Whiticar MJ (1999) Carbon and hydrogen isotope systematics of bacterial formation and oxidation of methane. Chem Geol 161:291–314

Whiticar MJ, Faber E (1986) Methane oxidation in sediment and water column environments—isotope evidence. Org Geochem 10:759–768

Wiedicke M, Sahling H, Delisle G, Faber E, Neben S, Beiersdorf H, Marchig V, Weiss W, von Mirbach N, Afiat A (2002) Characteristics of an active vent in the fore-arc basin of the Sunda Arc, Indonesia. Mar Geol 184:121–141